Rapid Communications

Crossover of correlation functions near a quantum impurity in a Tomonaga-Luttinger liquid

Chung-Yu Lo (羅中佑),[1] Yoshiki Fukusumi (福住吉喜),[2] Masaki Oshikawa (押川正毅),[2]
Ying-Jer Kao (高英哲),[3,4,*] and Pochung Chen (陳柏中)[1,4,†]

[1]*Department of Physics, National Tsing Hua University, Hsinchu 30013, Taiwan*
[2]*Institute for Solid State Physics, University of Tokyo, Kashiwa 277-8581, Japan*
[3]*Department of Physics, National Taiwan University, Taipei 10607, Taiwan*
[4]*National Center for Theoretical Sciences, Hsinchu 30013, Taiwan*

(Received 24 May 2018; revised manuscript received 22 October 2018; published 7 March 2019)

An impurity in a Tomonaga-Luttinger liquid leads to a crossover between the short- and long-distance regime which describes many physical phenomena. However, a calculation of the entire crossover of correlation functions over different length scales has been difficult. We develop a powerful numerical method based on the infinite density matrix renormalization group. By utilizing infinite boundary conditions we can obtain correlation functions within a finite-size window that contains the impurity. For the $S = 1/2$ chain, we demonstrate that a full crossover can be precisely obtained, and that their limiting behaviors show a good agreement with field-theory predictions.

DOI: 10.1103/PhysRevB.99.121103

In one-dimensional (1D) systems, even weak Coulomb interactions have dramatic effects and the Fermi-liquid theory describing their higher-dimensional counterparts breaks down. This results in a Tomonaga-Luttinger liquid (TLL) [1,2], which is simply a relativistic free boson field theory. The TLL behaviors have been experimentally demonstrated in carbon nanowires [3], allowing for further studies of the electron transport in 1D quantum wires. On the theory side, there exists a plethora of powerful analytical and numerical methods available to study the behavior of 1D systems. Analytical tools such as bosonization, conformal field theory (CFT), and the renormalization group (RG) can be employed to analyze the physical properties of TLL [2,4,5].

An important class of problems is the effects of a quantum impurity on a TLL [6–16]. In the simplest setting, Kane and Fisher have shown that a single quantum impurity affects the transport property of the TLL in an essential way [6,7]: When the interaction is attractive, the system renormalizes to a fixed point corresponding to a single fully connected wire. When the interaction is repulsive, however, the system renormalizes to two disconnected wires. An equivalent problem was also studied in a context of quantum spin chains [17]. In terms of CFT, a RG fixed point of the impurity problem is associated to a conformally invariant boundary condition (CIBC) [18]. Thus the first question in the impurity problem is the classification of CIBCs. While nontrivial CIBCs appear in various settings [19,20], only the simple Dirichlet and Neumann boundary conditions of the free boson field theory are relevant for the original Kane-Fisher problem (a single quantum impurity) in a spinless single-channel interacting TLL. For each CIBC, correlation functions can be calculated with boundary CFT techniques. However, the system is renormalized to the low-energy/large-distance (infrared, IR) fixed point only asymptotically. In order to describe various observable properties, such as finite-temperature properties, we need to describe the RG flow towards the IR fixed point, not just the CIBC corresponding to the IR fixed point. The system is often renormalized close to a high-energy/short-distance (ultraviolet, UV) fixed point first, before flowing towards the IR fixed point. In such a case, the finite-energy/finite-distance properties can be described as a crossover between the UV and IR fixed points. The crossover phenomena cannot be dealt with boundary CFT techniques alone. In some cases, the crossover of a physical quantity can be exactly obtained in terms of an integrable boundary RG flow [21]. Nevertheless, for more general quantities, and for other settings, a numerical approach is indispensable to describe the crossover.

In general, it is difficult to simulate 1D (boundary) critical systems, of which the TLL is an example, because large system sizes are required to capture the asymptotic behavior. Lo *et al.* [22] use a scale-invariant tensor network to directly extract scaling operators and scaling dimensions for both bulk and boundary CFTs. Although the method can successfully describe the physics at the IR fixed point, it cannot probe the UV to IR RG flow. Rahmani *et al.* [23,24] perform a conformal mapping of the wire junction to a finite strip so that a finite-size density matrix renormalization group (DMRG) calculation can be carried out. However, an *ad hoc* mirror boundary condition has to be added. Furthermore, conformal mapping makes it necessary to use the chord distance, instead of the direct site distance. It is therefore difficult to probe short-distance and crossover behavior using this approach. An improved numerical method is hence called for.

In this Rapid Communication, we present a numerical method based on an infinite DMRG (iDMRG) scheme that allows us to directly simulate the junction of semi-infinite TLL wires via the infinite boundary condition (IBC) and study

*yjkao@phys.ntu.edu.tw
†pcchen@phys.nthu.edu.tw

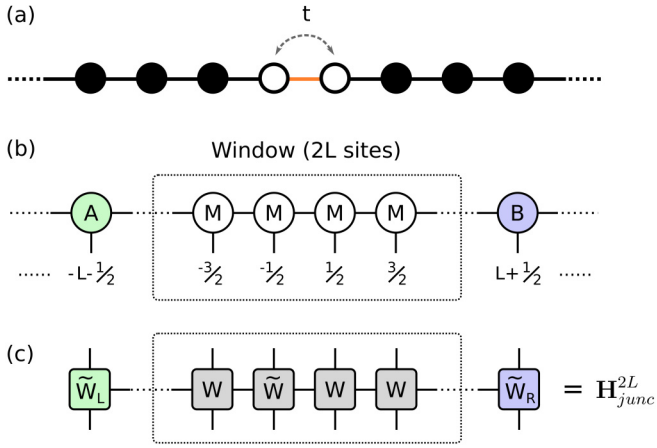

FIG. 1. (a) Sketch of the junction with a link of strength t. (b) iMPS diagram for $|\Psi\rangle^{G,2L}_{\rm junc}$. (c) MPO diagram for $H^{2L}_{\rm junc}$.

the crossover from the impurity site to the long length scale. We are able to obtain various correlation functions which are in agreement, at both the short and long length scales, with those obtained by the boundary perturbation theory based on bosonization [25–29].

We start from two semi-infinite wires of spinless electrons, which are connected by a link of strength t to form the junction as sketched in Fig. 1(a). Using the Jordan-Wigner transformation, the wire and the link Hamiltonians can be written in terms of $S = 1/2$ operators as

$$H_{\rm wires} = \sum_{i \in \mathcal{Z}^{>} + 1/2} -(S^+_{\pm i} S^-_{\pm(i+1)} + \text{H.c.}) + V S^z_{\pm i} S^z_{\pm(i+1)}, \tag{1}$$

where i is a positive half-integer and

$$H_{\rm link} = -t(S^+_{-1/2} S^-_{1/2} + S^-_{-1/2} S^+_{1/2}), \tag{2}$$

while the junction Hamiltonian is $H_{\rm junc} = H_{\rm wires} + H_{\rm link}$. We also define a bulk Hamiltonian as

$$H_{\rm bulk} = \sum_{i \in \mathcal{Z}+1/2} -\left(S^x_i S^x_{i+1} + S^y_i S^y_{i+1}\right) + V S^z_i S^z_{i+1}. \tag{3}$$

It differs from a $t = 1$ junction only by the interaction across the junction: $V S^z_{-1/2} S^z_{1/2}$. The semi-infinite wires and the bulk wire are both described by the TLL theory with the Luttinger parameter $g = \pi/[2\arccos(-V/2)]$. We will consider three interwire correlation functions: $\langle S^+_{-i} S^-_i \rangle$, $\langle S^z_{-i} S^z_i \rangle$, and $\langle J_{-i-1/2} J_{i+1/2} \rangle$. Here, the current operator is defined as $J_{i+1/2} \equiv -i(S^+_i S^-_{i+1} - S^-_i S^+_{i+1})$.

To find the ground state of $H_{\rm junc}$, we start from $H_{\rm bulk}$ and assume its ground state is a translationally invariant infinite matrix product state (iMPS),

$$\begin{aligned} |\Psi\rangle^G_{\rm bulk} &= \sum_{\{s_i\}} \cdots \lambda \Gamma^{s_{i-1}} \lambda \Gamma^{s_i} \lambda \Gamma^{s_{i+1}} \lambda \Gamma^{s_{i+2}} \cdots |\mathbf{s}\rangle \\ &= \sum_{s_i} \cdots A^{s_{i-1}} A^{s_i} \lambda B^{s_i} B^{s_{i+1}} \cdots |\mathbf{s}\rangle, \end{aligned} \tag{4}$$

where $|\mathbf{s}\rangle = |\ldots s_{i-1}, s_i, s_{i+1}, s_{i+2} \ldots\rangle$ and s_i are the local spin bases. Furthermore, $\Gamma^s = \Gamma$ are site-independent $d \times D \times D$ tensors and λ is a $D \times D$ diagonal matrix, where $d = 2$ is the dimension of the local Hilbert space on a single site and D is the virtual bond dimension. The second line corresponds to the mixed canonical form with $A^s = A = \lambda\Gamma$ and $B^s = B = \Gamma\lambda$. Here, A and B satisfy the left and right canonical form constraints, respectively. They can be obtained by optimizing $|\Psi\rangle^G_{\rm bulk}$ with $H_{\rm bulk}$ via conventional iDMRG algorithms. Due to the presence of the impurity, the translational invariance is broken and $|\Psi\rangle^G_{\rm bulk}$ is not a good ansatz for the ground state of $H_{\rm junc}$. However, since $H_{\rm junc}$ differs from $H_{\rm bulk}$ only at the impurity sites, we expect that far away from these sites the ground states of $H_{\rm junc}$ and $H_{\rm bulk}$ should resemble each other locally. We hence assume that there is a finite window of size $2L$ with sites $i \in [-L + \frac{1}{2}, \ldots, L - \frac{1}{2}]$ within which the ground states of $H_{\rm junc}$ and $H_{\rm bulk}$ differ, while outside this window they are described by the same matrices. This leads to the following iMPS ansatz for the ground state of $H_{\rm junc}$,

$$|\Psi\rangle^{G,2L}_{\rm junc} = \sum_{s_i} \cdots A^{s_{-\tilde{L}-1}}][M^{s_{-\tilde{L}}} \cdots M^{s_{\tilde{L}}}][B^{s_{\tilde{L}+1}} \cdots |\mathbf{s}\rangle, \tag{5}$$

where $\tilde{L} = L - 1/2$ as sketched in Fig. 1(b). Here, L is an adjustable parameter that can be easily enlarged, and the M matrices are optimized with an effective Hamiltonian as described below.

Starting from $H_{\rm bulk}$ in the form of matrix product operators (MPOs) [30],

$$H_{\rm bulk} = \cdots W_{-L-\frac{1}{2}} W_{-L+\frac{1}{2}} \cdots W_{-\frac{1}{2}} W_{\frac{1}{2}} \cdots W_{L-\frac{1}{2}} W_{L+\frac{1}{2}} \cdots, \tag{6}$$

where the $W_i = W$ is site independent. The effective Hamiltonian of the finite window reads

$$H^{2L}_{\rm junc} = \widetilde{W}_{\mathcal{L}} W_{-L+\frac{1}{2}} \cdots \widetilde{W}_{-\frac{1}{2}} W_{\frac{1}{2}} \cdots W_{L-\frac{1}{2}} \widetilde{W}_{\mathcal{R}}, \tag{7}$$

as sketched in Fig. 1(c). Here,$W_{-1/2}$ is replaced by $\widetilde{W}_{-1/2}$ to represent $H_{\rm link}$. Furthermore, the left and right IBCs, $\widetilde{W}_{\mathcal{L}}$ and $\widetilde{W}_{\mathcal{R}}$, are constructed from the left and right dominant eigenvectors of the generalized transfer matrices $T_{\mathcal{L}} = \sum_{ss'} \langle s|W|s'\rangle A^{s'\dagger} A^s$ and $T_{\mathcal{R}} = \sum_{ss'} \langle s|W|s'\rangle B^s B^{s\dagger}$, respectively [31]. Here, the IBCs are used to represent the semi-infinite extensions of the bulk system to the left and right. In this way, we reduce an infinite-size problem to an effective finite-size one [32]. Once $H^{2L}_{\rm junc}$ is obtained, one can use conventional finite-size MPS/DMRG algorithms to optimize the M matrices. Also, with the left- and right-canonical conditions satisfied by the A and B matrices, correlation functions within the window can be calculated using only the M matrices.

When $g > 1$, at the IR limit the system is renormalized to a single wire with the same Luttinger parameter. For a weaker link (smaller t), we expect that it would take a longer distance for the system to heal from the perturbation due to the impurity. Figure 2 shows $\langle S^+_{-i} S^-_i \rangle$, $\langle S^z_{-i} S^z_i \rangle$, and $\langle J_{-i-1/2} J_{i+1/2} \rangle$ correlation functions for junctions with $g = 1.5$ and various t's and the bulk wire. We observe that at the IR limit all correlation functions merge into their bulk counterparts. This confirms that asymptotically the system is renormalized to a single defect-free wire.

When $g < 1$, in contrast, we expect that in the IR limit the system is renormalized into two disconnected semi-infinite wires. For nonzero t, we still expect the correlation functions to decay as a power law, but with exponents that are larger than

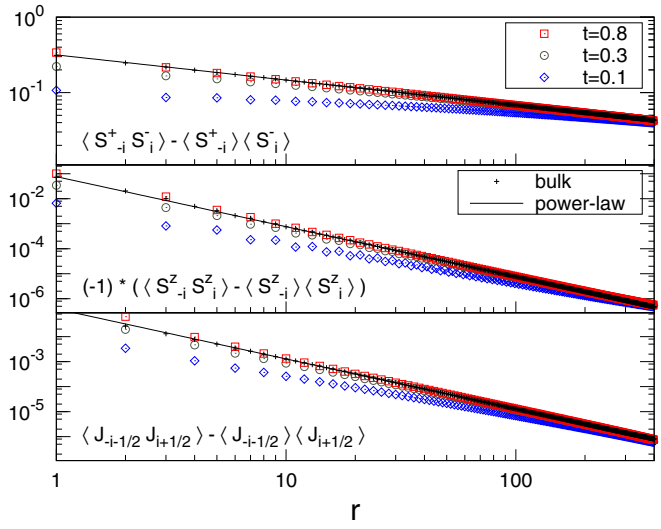

FIG. 2. $\langle S^+_{-i}S^-_i\rangle$, $\langle S^z_{-i}S^z_i\rangle$, and $\langle J_{-i-1/2}J_{i+1/2}\rangle$ correlation functions for $g = 1.5$. Data for the bulk and junctions with $t = 0.1$, 0.3, and 0.8 are plotted. Solid lines are power-law fittings to the bulk data with bulk exponents from bosonization (cf. Table I).

the bulk counterparts. In Fig. 3, we plot the same correlation functions for $g = 0.6$ and $t = 0.1$ and 0.01 and the bulk wire. A scaling prefactor of t^{-1} or t^{-2} is included to collapse the curves with different t's. It is clear that the correlators in the IR limit decay faster than their bulk counterparts, supporting the picture that at the IR limit the system is renormalized into broken wires.

To further understand the behavior of these correlation functions in both the UV and the IR limits, we use boundary perturbation theory to determine the exponents of the power laws. To the leading order, we derive the exponents of

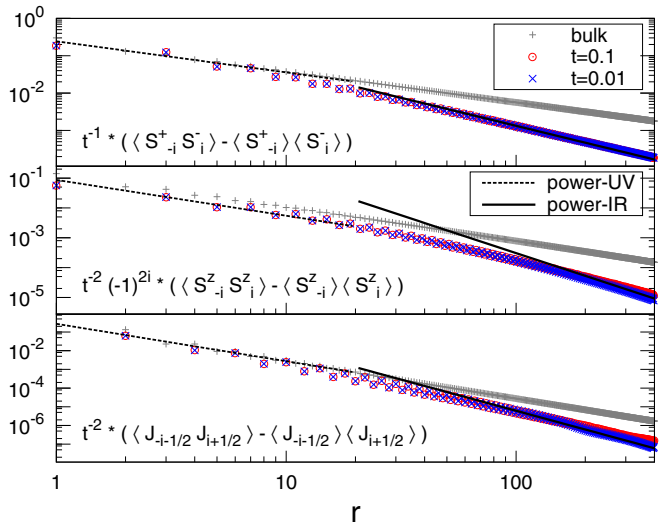

FIG. 3. Rescaled $\langle S^+_{-i}S^-_i\rangle$, $\langle S^z_{-i}S^z_i\rangle$, and $\langle J_{-i-1/2}J_{i+1/2}\rangle$ correlation functions for $g = 0.6$. Data for the bulk and junctions with $t = 0.1$ and 0.01 are plotted. Solid (dotted) lines are power-law fittings to the long- (short-) distance data with IR (UV) exponents from bosonization, except that for $\langle S^+_{-i}S^-_i\rangle$ at the IR limit the prefactor $C_0 = 1.330$ from bosonization is used [32] (cf. Table I).

the uniform and staggered part of the correlation functions, respectively. In the bosonization framework, the system is described by the TLL with the Lagrangian density

$$\mathcal{L} = \frac{1}{2\pi g}(\partial_\mu\phi)^2. \tag{8}$$

In the leading orders, the spin and current operators are expressed as [2,33,34]

$$S^-_j \sim e^{-i\theta}\sum_{n=0}^{\infty}[b_{2n}\cos(4n\phi) + (-1)^j b_{2n+1}\sin[2(2n+1)\phi]], \tag{9}$$

$$S^z_j \sim -\frac{1}{\pi}\frac{\partial\phi}{\partial x} + \sum_{n=0}^{\infty}(-1)^j a_{2n+1}\sin[2(2n+1)\phi], \tag{10}$$

$$J_j = i(S^+_{j+1}S^-_j - S^+_j S^-_{j+1}) \sim \frac{gv}{\pi}\frac{\partial\theta}{\partial x}, \tag{11}$$

where a_n and b_n are constants. Here, θ is the dual field of ϕ defined by $\theta \equiv \frac{1}{g}(\phi_L - \phi_R)$, where $\phi = \phi_L(\bar z) + \phi_R(z)$ is the chiral decomposition into left/right movers with $z = x + i\tau = x - t$ and $\bar z = x - i\tau$. While the constants a_n and b_n are nonuniversal, a few of them are determined exactly for the XXZ chain from the Bethe ansatz solution [35].

The geometry is a half plane with the interaction on the line $x = 0$. In the limit $t = 0$, the system is two decoupled half chains. We can then introduce the link Eq. (2) between the two decoupled chains as a perturbation. Let us consider the correlation function $\langle S^+_{-i}S^-_i\rangle$, across the link. Obviously it vanishes when $t = 0$. In the first order of t, the correlation function is given as

$$t\int d\tau\left[\frac{1}{2}\langle S^+_{-i}(0)S^-_{-\frac{1}{2}}(\tau)\rangle_0\langle S^+_{\frac{1}{2}}(\tau)S^-_i(0)\rangle_0\right], \tag{12}$$

where $\langle\,\rangle_0$ represents the ground-state expectation value in the decoupled chains with open boundary conditions.

In terms of the field theory, the open boundary condition corresponds to the Dirichlet boundary condition on ϕ. Thus the correlation functions in the decoupled chain can be calculated using Eq. (9), as discussed in Refs. [32,34],

$$\langle S^+_{-i}S^-_i\rangle = t\left[C_0 r^{-(\frac{3}{2g}-1)} + C_0'(-1)^r r^{-(\frac{3}{2g}+2g-1)} + \cdots\right], \tag{13}$$

where $i \in \mathcal{Z}^{\geqslant} + \frac{1}{2}$, $r = 2i$, and C_0, C_0' are constants. The prefactor C_0 is given as

$$C_0 = \frac{1}{2v}b_0{}^2(b_0 + 2^{-g}b_1 - 2^{-4g}b_2 - 2^{-9g}b_3\cdots)^2 \times 2^{5/(2g)-1}\frac{\sqrt{\pi}\Gamma\left(\frac{1}{g}-\frac{1}{2}\right)}{\Gamma\left(\frac{1}{g}\right)}. \tag{14}$$

It should be noted that the prefactor C_0 has contributions from all b_n's, in contrast to the bulk correlation function. However, terminating the sum at the first few terms would give a good approximation. The values of b_0 and b_1 are known exactly for the XXZ chain, and b_2 can be estimated by a fitting of the correlation functions in the open chain. We thus estimated C_0 using Eq. (14) including up to b_2 [32]. Similarly, we find

$$\langle S^z_{-i}S^z_i\rangle = t^2\left[C_0 r^{-(\frac{2}{g})} + C_0'(-1)^r r^{-(2g+\frac{2}{g}-2)}\right], \tag{15}$$

TABLE I. Dominant exponents for each correlation function.

	$g>1$			$g<1$		
	Bulk IR	IR	UV	Bulk IR	IR	UV
$\langle S^+_{-i}S^-_i\rangle$	$\frac{1}{2g}$	$\frac{1}{2g}$	$\frac{3}{2g}-1$	$\frac{1}{2g}$	$\frac{3}{2g}-1$	$\frac{1}{2g}$
$\langle S^z_{-i}S^z_i\rangle$	2	2	$\frac{2}{g}$	$2g$	$2g+\frac{2}{g}-2$	$2g$
$\langle J_{-i-1/2}J_{i+1/2}\rangle$	2	2	$\frac{2}{g}$	2	$\frac{2}{g}$	2

where $r=2i$ and

$$\langle J_{-i-1/2}J_{i+1/2}\rangle = t^2 C_0 r^{-\frac{2}{g}}, \tag{16}$$

where $r=2i+1$. Unfortunately, the prefactors of these leading terms at $O(t^2)$ cannot be determined analytically.

These results in the lowest order of the perturbation theory describe the IR behavior for $g<1$ and the UV behavior for $g>1$. We find that for $g>1$, the uniform part always dominates and the UV exponents are $3/2g-1$, $2/g$, and $2/g$, respectively. In contrast, for $g<1$ the staggered part of the $\langle S^z_{-i}S^z_i\rangle$ becomes dominant and the IR exponents become $3/2g-1$, $2g+2/g-2$, and $2/g$, respectively.

The case of a weak barrier (small $1-t$), on the other hand, corresponds to the free boundary condition. For this case we regard the junction as a defect in CFT with

$$H_{\text{barrier}} = (1-t)(S^+_{-1/2}S^-_{1/2}+S^-_{-1/2}S^+_{1/2}) - VS^z_{-1/2}S^z_{1/2}. \tag{17}$$

We evaluate this defect by using the operator product expansion for CFT. By the usual perturbation theory, we find

$$\langle S^+_{-i}S^-_i\rangle = C_0 r^{-\frac{1}{2g}} + C_0'(-1)^r r^{-\frac{1}{2g}+2g}, \tag{18}$$

$$\langle S^z_{-i}S^z_i\rangle = C_0 r^{-2} + C_0' r^{-2g}, \tag{19}$$

where $i\in\mathcal{Z}^{\geqslant}+\frac{1}{2}$ and $r=2i$, and

$$\langle J_{-i-1/2}J_{i+1/2}\rangle = C_0 r^{-2}, \tag{20}$$

where $r=2i+1$. These results describe the IR behavior for $g>1$ and the UV behavior for $g<1$. We find that for $g>1$, the uniform part always dominates and the IR exponents are $1/2g$, 2, and 2, respectively. In contrast, for $g<1$ the staggered part of the $\langle S^z_{-i}S^z_i\rangle$ dominates and the UV exponents are $1/2g$, $2g$, and 2. These results also describe the IR behavior for a single bulk TLL wire. In Table I, we summarize the dominant exponent for each correlation function [32].

We now compare the numerical results against these power laws. Figure 2 shows the fit of the bulk correlation functions to Eqs. (18)–(20) for the case of an attractive interaction $g=1.5$. The numerical results confirm that in the IR limit all correlation functions decay with the corresponding bulk exponents. Also, we see that for smaller t, it takes a longer distance for the system to reach the IR limit, indicating it needs more steps to renormalize away the impurity.

In Fig. 3 we compare the numerical results against the bosonization results for the case of a repulsive interaction $g=0.6$. At the IR limit the system is renormalized into two disconnected semi-infinite wires, which corresponds to the Dirichlet boundary condition. Very small values of $t=0.1$ and 0.01 are used to probe the IR behavior. We observe that the crossover of the correlation functions is consistent with the field theoretical prediction as in Table I. Remarkably, the prefactor C_0 of the $\langle S^+S^-\rangle$ correlation function in the IR regime agrees very well with the bosonization prediction [32]. This demonstrates the accuracy of the present method applied to long-distance correlation functions of the impurity problem.

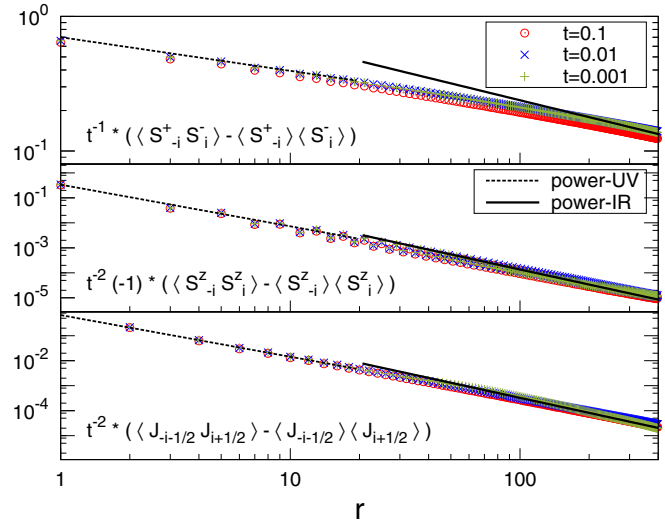

FIG. 4. Rescaled $\langle S^+_{-i}S^-_i\rangle$, $\langle S^z_{-i}S^z_i\rangle$, and $\langle J_{-i-1/2}J_{i+1/2}\rangle$ correlation functions for $g=1.2$. Data for junctions with $t=0.1$, 0.01, and 0.001 are plotted. Solid (dotted) lines are power-law fittings to the long- (short-) distance data with IR (UV) exponents from bosonization, except that for $\langle S^+_{-i}S^-_i\rangle$ at the UV limit the prefactor $C_0=0.701$ from bosonization is used [32] (cf. Table I).

On the other hand, while small $1-t$ is assumed in the derivation of Eqs. (18)–(20), the exponents describe well the numerical results at short distances even when t is small. Moreover, the same scaling prefactors also result in a data collapse at short distances. Interestingly, this indicates that near the junction, the system does not know which fixed point it should renormalize into, and the correlation in the short distance resembles that in the bulk, scaled with the junction strength t.

Finally, we analyze the UV behavior for the case of $g>1$. Figure 4 plots rescaled correlation functions for the case of $g=1.2$ and various extremely small t's in order to expose the UV regime. In this limit, we are able to fit the numerical results to the boundary perturbation theory results with the Dirichlet boundary condition before crossing over to the long-distance behavior. Both the exponents and scaling prefactor agree well. In Fig. 4 we also show the power-law fitting in the IR limit and the crossover from UV to IR exponents is clearly observed.

In summary, we present a robust and powerful numerical method to study a junction between two quantum wires. This method allows one to study numerically the crossover of correlation functions near a quantum impurity between

the short- and long-distance regimes, as demonstrated by the perfect fit of the UV and IR behaviors between the numerical and bosonization results. This may lead to further explorations of the crossover behavior from UV to IR [36]. We also emphasize that this method is also applicable to a more general class of interesting problems, such as the Y junction for TLL leads [20,23,24], TLL leads with different Luttinger parameters [37], and junctions with spin-1/2 interacting fermion leads [38].

This work was supported by the MOST of Taiwan under Grants No. 105-2112-M-002-023-MY3, No. 104-2628-M-007-005-MY3, and No. 104-2112-M-002-022-MY3, and by MEXT/JSPS KAKENHI Grants No. JP16K05469 and No. JP17H06462 of Japan. C.-Y.L. thanks Shuai Yin for helpful discussions. Y.-J.K. thanks the hospitality of ISSP, University of Tokyo, where part of the work was done. The numerical calculation was done using the Uni10 tensor network library [39].

[1] S. Tomonaga, Prog. Theor. Phys. **5**, 544 (1950); J. M. Luttinger, J. Math. Phys. **4**, 1154 (1963).
[2] T. Giamarchi, *Quantum Physics in One Dimension* (Oxford University Press, Oxford, U.K., 2004).
[3] D. Laroche, G. Gervais, M. P. Lilly, and J. L. Reno, Science **343**, 631 (2014); H. Ishii, H. Kataura, H. Shiozawa, H. Yoshioka, H. Otsubo, Y. Takayama, T. Miyahara, S. Suzuki, Y. Achiba, M. Nakatake, T. Narimura, M. Higashiguchi, K. Shimada, H. Namatame, and M. Taniguchi, Nature (London) **426**, 540 (2003); Z. Yao, H. W. C. Postma, L. Balents, and C. Dekker, *ibid.* **402**, 273 (1999); N. Y. Kim, P. Recher, W. D. Oliver, Y. Yamamoto, J. Kong, and H. Dai, Phys. Rev. Lett. **99**, 036802 (2007); H. W. C. Postma, M. de Jonge, Z. Yao, and C. Dekker, Phys. Rev. B **62**, R10653 (2000).
[4] J. L. Cardy, Conformal field theory and statistical mechanics, in *Exact Methods in Low-Dimensional Statistical Physics and Quantum Computing*, edited by J. Jesperson *et al.*, Lecture Notes of the Les Houches Summer School LXXXIX, 2008 (Oxford University Press, Oxford, U.K., 2010).
[5] I. Affleck, Quantum impurity problems in condensed matter physics, in *Exact Methods in Low-Dimensional Statistical Physics and Quantum Computing* (Ref. [4]).
[6] C. L. Kane and M. P. A. Fisher, Phys. Rev. Lett. **68**, 1220 (1992); Phys. Rev. B **46**, 15233 (1992).
[7] A. Furusaki and N. Nagaosa, Phys. Rev. B **47**, 4631 (1993).
[8] K. A. Matveev, D. Yue, and L. I. Glazman, Phys. Rev. Lett. **71**, 3351 (1993).
[9] E. Wong and I. Affleck, Nucl. Phys. B **417**, 403 (1994).
[10] C. Rylands and N. Andrei, Phys. Rev. B **94**, 115142 (2016).
[11] Z. Shi and I. Affleck, Phys. Rev. B **94**, 035106 (2016).
[12] F. Lesage and H. Saleur, Nucl. Phys. B **546**, 585 (1999).
[13] F. Lesage, H. Saleur, and S. Skorik, Phys. Rev. Lett. **76**, 3388 (1996).
[14] A. Koutouza, F. Lesage, and H. Saleur, Phys. Rev. B **68**, 115422 (2003).
[15] P. Fendley, A. W. W. Ludwig, and H. Saleur, Phys. Rev. Lett. **75**, 2196 (1995).
[16] R. Egger, H. Grabert, A. Koutouza, H. Saleur, and F. Siano, Phys. Rev. Lett. **84**, 3682 (2000).
[17] S. Eggert and I. Affleck, Phys. Rev. B **46**, 10866 (1992).
[18] H. Saleur, in *Exact Methods in Low-dimensional Statistical Physics and Quantum Computing*, edited by J. Jacobsen, S. Ouvry, V. Pasquier, D. Serban, and L. Cugliandol, Lecture Notes of the Les Houches Summer School, Vol. 89 (Oxford University Press, 2008).
[19] I. Affleck and A. Ludwig, Nucl. Phys. B **352**, 849 (1991).
[20] M. Oshikawa, C. Chamon, and I. Affleck, J. Stat. Mech. (2006) P02008.
[21] P. Fendley, A. W. W. Ludwig, and H. Saleur, Phys. Rev. Lett. **74**, 3005 (1995).
[22] Y.-L. Lo, Y.-D. Hsieh, C.-Y. Hou, P. Chen, and Y.-J. Kao, Phys. Rev. B **90**, 235124 (2014).
[23] A. Rahmani, C.-Y. Hou, A. E. Feiguin, C. Chamon, and I. K. Affleck, Phys. Rev. Lett. **105**, 226803 (2010).
[24] A. Rahmani, C.-Y. Hou, A. E. Feiguin, M. Oshikawa, C. Chamon, and I. K. Affleck, Phys. Rev. B **85**, 045120 (2012).
[25] V. Fateev, S. L. Lukyanov, A. B. Zamolodchikov, and A. B. Zamolodchikov, Phys. Lett. B **406**, 83 (1997).
[26] P. Fendley and H. Saleur, Phys. Rev. Lett. **81**, 2518 (1998).
[27] P. Fendley, Adv. Theor. Math. Phys. **2**, 987 (1998).
[28] P. Fendley and H. Saleur, Phys. Rev. Lett. **75**, 4492 (1995).
[29] A. Furusaki and T. Hikihara, Phys. Rev. B **58**, 5529 (1998).
[30] U. Schollwoeck, Ann. Phys. **326**, 96 (2011); I. P. McCulloch, J. Stat. Mech. (2007) P10014.
[31] H. N. Phien, G. Vidal, and I. P. McCulloch, Phys. Rev. B **86**, 245107 (2012).
[32] See Supplemental Material at http://link.aps.org/supplemental/10.1103/PhysRevB.99.121103 for details on the infinite boundary condition, and boundary perturbation theory, which includes Refs. [40–46].
[33] S. L. Lukyanov and V. Terras, Nucl. Phys. B **654**, 323 (2003).
[34] T. Hikihara and A. Furusaki, Phys. Rev. B **69**, 064427 (2004).
[35] S. Lukyanov and A. Zamolodchikov, Nucl. Phys. B **493**, 571 (1997).
[36] T. T. Wu, B. M. McCoy, C. A. Tracy, and E. Barouch, Phys. Rev. B **13**, 316 (1976).
[37] C.-Y. Hou, A. Rahmani, A. E. Feiguin, and C. Chamon, Phys. Rev. B **86**, 075451 (2012).
[38] C.-Y. Hou and C. Chamon, Phys. Rev. B **77**, 155422 (2008).
[39] Y.-J. Kao, Y.-D. Hsieh, and P. Chen, J. Phys.: Conf. Ser. **640**, 012040 (2015); Uni10 tensor network library, https://uni10.gitlab.io/.
[40] L. Michel and I. P. McCulloch, arXiv:1008.4667.
[41] H. N. Phien, G. Vidal, and I. P. McCulloch, Phys. Rev. B **88**, 035103 (2013).
[42] A. Milsted, J. Haegeman, T. J. Osborne, and F. Verstraete, Phys. Rev. B **88**, 155116 (2013).
[43] V. Zauner-Stauber, M. Ganahl, H. G. Evertz, and T. Nishino, J. Phys.: Condens. Matter **27**, 425602 (2015).
[44] J. Sato, M. Shiroishi, and M. Takahashi, Nucl. Phys. B **729**, 441 (2005).
[45] N. A. Slavnov, Theor. Math. Phys. **150**, 259 (2007).
[46] J. Sato and M. Shiroishi, J. Phys. A **40**, 8739 (2007).